Second Conference on Smart Monitoring,
Assessment and Rehabilitation of Civil Structures

SMAR 2013

Comparison of fibre optic sensors and digital image correlation for strain measurement in reinforced concrete beams

Danielle DeRosa[1], Mark F. Green[1], Neil A. Hoult[1], and Andy W. Take[1]

[1] Department of Civil Engineering, Queen's University, Kingston, Canada

ABSTRACT: Currently, monitoring projects for civil structures rely heavily on conventional vibrating wire strain gauges, which while robust and accurate are also expensive and offer only discrete strain data points. As infrastructure around the world continues to deteriorate, engineers tasked with assessing these assets require more information about structural performance and data to validate the results of numerical assessments. Two technologies that offer tremendous potential in this regard are distributed fibre optic sensors (FOS) and digital image correlation (DIC). However, these systems require validation against conventional strain measurement techniques in order to ensure that they provide the required accuracy. The research presented compares measurements made with both FOS and DIC to results from conventional strain gauges on reinforced concrete beams during loading in the linear-elastic range. Two beams are tested in four point bending with all three sensor systems installed in the shear span where linear-elastic beam behaviour is expected. The strain results are presented for all three sensor systems. Good agreement between the FOS and strain gauges is observed. Out of plane movement is determined to be a major potential source of error for DIC measurements. Recommendations are made for procedures to achieve accurate measurements with FOS and DIC in field applications.

1 INTRODUCTION

Many reinforced concrete structures in North America are reaching the end of their service life. Visual inspections are an important part of the assessment process but they rely on the knowledge of the inspector, are prone to human error, and are inherently subjective (Graybeal et al., 2003). Weak points in a structure can go unnoticed, are hidden internally, or are inaccurately identified. One approach to overcome these limitations is to install a sensor network. Recent advances make it possible to remotely gather comprehensive data about a structure's performance using a variety of sensor technologies. Fibre optic strain sensors (FOS) and digital image analysis techniques (commonly referred to as digital image correlation - DIC) are two of the recent breakthrough technologies that will be discussed in this paper. However, little research has been done to calibrate these systems against more conventional technologies to ensure they produce accurate measurements. One of the critical areas for further research is in the verification and calibration of both FOS and DIC systems for strain measurement.

This paper will aim to determine the accuracy of two new sensor technologies compared to electrical resistance strain gauges. The next section provides a background on the FOS and DIC techniques, followed by a detailed explanation of the experimental program. The results are presented and discussed. Lastly, the paper will give some conclusions and recommendations for future work.

2 BACKGROUND

2.1 Fibre Optic Strain Sensors

Fibre optic strain sensors (FOS) are now commercially available for monitoring civil infrastructure assets (Lanticq et al., 2009). Unlike traditional sensors (e.g., electrical resistance strain gauges), FOS are quite robust because they do not drift over time, resist electromagnetic interference, are corrosion resistant, and have a relatively long life-cycle (Casas and Cruz, 2003). The sensors are able to monitor strain and temperature, and can have similar accuracy to conventional strain gauges (Casas and Cruz, 2003).

Discrete FOS, such as Fibre Bragg grating (FBG) sensors, have been around for over 20 years and have been successfully used to monitor reinforced concrete bridges (e.g. Tennyson et al., 2001). Recently, distributed sensing technologies have been introduced. When assessing infrastructure, a distributed sensing system would provide strain or temperature measurements along the full length of an optical fibre and thus potentially allow for the detection of localized deterioration. Because distributed FOS is a relatively new technology, limited applications in civil engineering structures have been demonstrated to date (e.g. Bao et al., 2001). Therefore this technology will be further investigated in this research.

Distributed FOS works by pulsing light through an optical fibre. A small portion of that light is backscattered due to imperfections in the cable. Several different technologies exist that measure the components of the backscattered light and convert these readings into strain or temperature measurements based on the properties of the fibre. Technologies include optical time domain reflectometry (OTDR), which uses the Rayleigh or Raman scatter (temperature only), Brillouin optical time domain reflectometry (BOTDR), and Brillouin optical time domain analysis (BOTDA) (Güemes et al., 2010).

Another available technology is called optical frequency domain reflectometry (OFDR). OFDR works by measuring changes in the frequency (due to attenuation mechanisms such as temperature, mechanical strain, or a break in the fibre) of the Rayleigh scatter as a function of the length of fibre (Kreger et al., 2006). By comparing OFDR measurements of a stressed optical fibre with reference measurements, strain or temperature can be obtained along up to 70 m of fibre with 10 mm spatial resolution with strain and temperature resolution as fine as 1 με and 0.1 °C (Luna Innovations Incorporated, 2009). In this study, the accuracy of the OFDR system will be explored to determine whether the stated accuracy can be achieved for reinforced concrete structures in a laboratory environment.

One of the major problems with FOS is the cross sensitivity to strain and temperature. Both strain and temperature induce a strain reading in the fibre optic cable and therefore these two variables must be separated to achieve accurate measurements of each variable. The main technique employed by previous researchers is the use of a ‘dummy sensor’, which is a portion of the optical fibre free from mechanical strain subjected to the same thermal environment as the structure of interest (e.g. Bourne-Webb et al., 2009 and Bao et al., 2001). This portion of fibre will detect only temperature effects, and thus this strain can be subtracted from the measured output of a fibre bonded to the structure to determine the mechanical strain.

2.2 Digital Image Correlation

Digital image correlation (DIC) works by comparing digital images of a deformed object to a digital image of the object before deformation. By tracking the location of a segment of an image known as a patch, from the reference image to the deformed image, a two-dimensional displacement field can be created for that object and the strain can be determined from the

displacement field. While electrical resistance strain gauges provide only discrete readings over a fixed gauge length, the DIC technique can provide a two-dimensional surface strain field using a single camera. Because strain gauges must be securely attached to the surface of the object, they are quite labour intensive to install and often cannot be reused. DIC, on the other hand, is a non-contact measurement technique and the camera can be reused.

For this research, a program developed by White et al. (2003) specifically for monitoring deformations of solids called *geoPIV* is used. *GeoPIV* does not require artificial targets in the various images to track displacements. Instead, a texture on the object under observation is required, often applied in the form of spray paint, to provide sufficient texture to each patch to distinguish it from the surrounding search area (Dutton et al., 2011). The image is divided into patches that are searched for in each subsequent deformed image over a predefined search zone. The degree of match is defined by calculating the normalized cross correlation of the test patch within the search zone, which allows the patch to be located to within one pixel. However, one-pixel accuracy is not acceptable for strain resolution. As a result, *geoPIV* implements a B-spline interpolation to determine the new location of a patch to the nearest sub-pixel. A thorough explanation of the program can be found in the literature (White et al., 2003; Lee et al., 2012).

Several researchers have used *geoPIV* to observe structural members under load. Thusyanthan et al. (2007) monitored strains and cracks in kaolin clay beams loaded in four-point bending using *geoPIV*. Bisby et al. (2007) investigated the use of *geoPIV* to quantify strain variation in concrete cylinders confined by fibre reinforced polymers. In each case the strains being monitored were siginificantly larger than those that would be expected in field applications and so the current work explores the accuracy of the technique at very low strains.

3 EXPERIMENTAL PROGRAM

The experimental program investigated the use of FOS and DIC to measure strain for two reinforced concrete beams during loading in the linear-elastic region. The results of the FOS and DIC analysis will be compared to strain gauge readings to determine the accuracy and precision of these two new technologies versus an accepted technology.

3.1 Specimen Design

The two beams had a cross-section measuring 200 mm by 400 mm as shown in Figure 1. The specimens were 4200 mm long and were tested in four point bending with a 1200 mm shear span as shown in Figure 2. The beam cross section consisted of two 10M bars as top reinforcement and two 20M bars as bottom reinforcement.

Table 1 provides the concrete properties for each beam tested. The theoretical cracking load listed in Table 1, was calculated using the modulus of rupture equation found in the *Design of Concrete Structures* (CSA A23.3, 2006), using the mean compressive strength obtained from the cylinder tests. The yield strength of the 10M rebar and 20M rebar was 478 MPa and 453 MPa respectively and the ultimate strength was 576 MPa and 563 MPa respectively, provided by the manufacturer. It is worth noting that the yield point was not reached during this experiment.

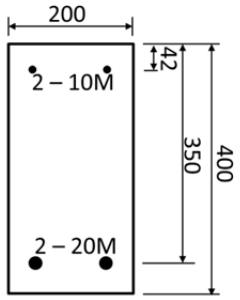

Figure 1: Beam cross section (dimensions in mm)

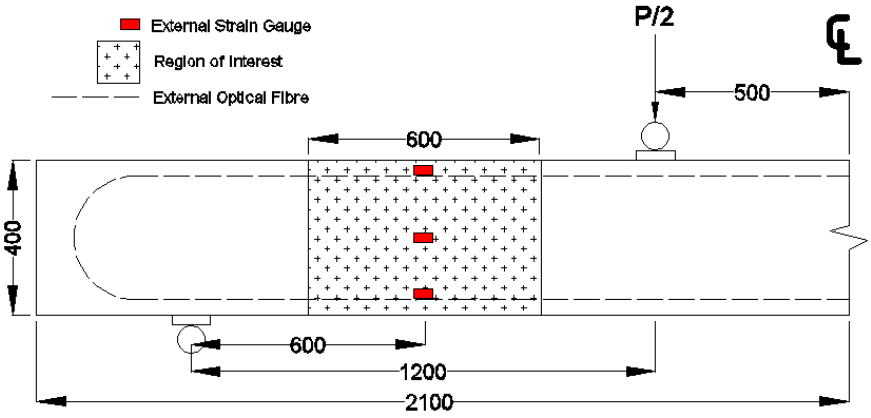

Figure 2: Beam instrumentation layout (dimensions in mm)

Table 1: Beam concrete properties

Beam	Compressive Strength (MPa)	Split Cylinder Strength (MPa)	Theoretical Cracking Load (*P*) (kN)
1	37	2.7	32
2	33	2.5	31

3.2 Instrumentation

The instrumentation layout is shown in Figure 2. Three external strain gauges with a 50.8 mm gauge length were adhered to each beam at varying heights at the centre of the shear span. An external fibre optic cable was adhered to the surface of the concrete beam, after grinding and cleaning of the concrete surface. A single mode fibre with a core diameter of 8.2 µm and an acrylic coating was used. The fibre optic analyser, an OBR 4600, was used to capture and later analyse the FOS readings. For the DIC monitoring, two cameras (Canon EOS Rebel T2i) using 18-55 mm adjustable lenses set to 55 mm on tripods were placed on either side of the beam focusing on the region of interest highlighted in Figure 2. Each camera was placed approximately 1400 mm away from the face of the beam. The testing frame for this experiment was in a small laboratory space that required the cameras to be placed close to the beam and that thus required a lens with a small focal length. This short distance to the specimen has a negative effect on the accuracy of the DIC technique as discussed elsewhere (Hoult et al., 2013). The surface was speckled with black spray paint to provide the required texture for DIC analysis.

3.3 Test Setup

The load was increased to 30 kN in load stages of 10 kN intervals. Loading beyond 30 kN is not discussed in this paper because it is no longer in the linear-elastic region, and any cracks forming near the strain gauges would cause inaccurate readings making verification and calibration of the new sensor systems with the strain gauges much more challenging. Fibre optic scans and DIC images were taken prior to loading to establish a reference and at each load stage. Both cameras were triggered remotely to simultaneously record an image every two seconds for a total of 10 images. The 10 images were later averaged together to decrease the error caused by camera jitter and lighting as discussed elsewhere (Hoult et al., 2013).

4 RESULTS

During the beam experiments, the beam specimen was tested on a reaction beam loaded with an adjustable actuator head. Therefore, there was a potential for the beam to be loaded eccentrically resulting in out of plane movement or rotation of the beam if it were not precisely centred in the testing frame. In order to detect any potential out of plane movement using DIC analysis, images were captured simultaneously on opposite sides of each beam as suggested by Hoult et al. (2013). A 64 by 64 pixel patch size was used to track displacements in the DIC analysis. Figure 3 displays the DIC patch layout and gauge lengths for side A and B of Beam 2.

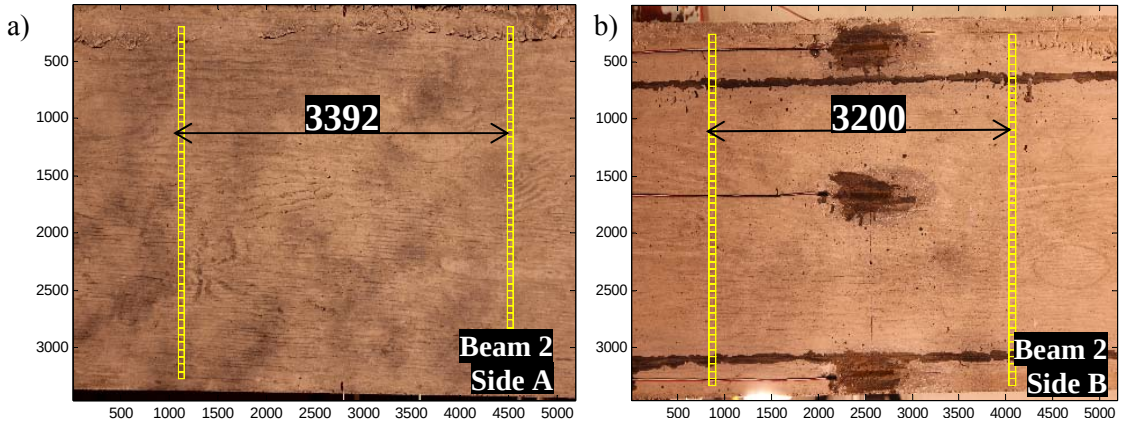

Figure 3: DIC patch layout and gauge lengths (in pixels) for Beam 2 a) side A and b) side B

Figure 4 shows the results of the DIC analysis for Beam 2. The strain profiles on either side of the beam are almost mirror images of each at each load stage. In addition, the strain values are much larger than what is expected. From these results, it is likely that the beam is rotating or translating out of plane. The large positive strains on side B indicate that the beam is rotating and translating towards side B, with the top of the beam moving closer to the camera than the bottom. As the beam moves closer to the camera, the magnification of the image is perceived by the DIC analysis as being the same as the patches moving farther apart, resulting in large tensile strains on side B and similarly large compressive strains on side A.

In order to compensate for this out of plane error, a single strain profile for each beam is obtained by taking a weighted average of the strain profile on side A and B at each load stage based on the distance between the camera lens and the surface of the beam. The results of Beam 1 and 2 are presented in Figure 5 where for simplicity, best fit lines of the strain profiles are used rather than the original data.

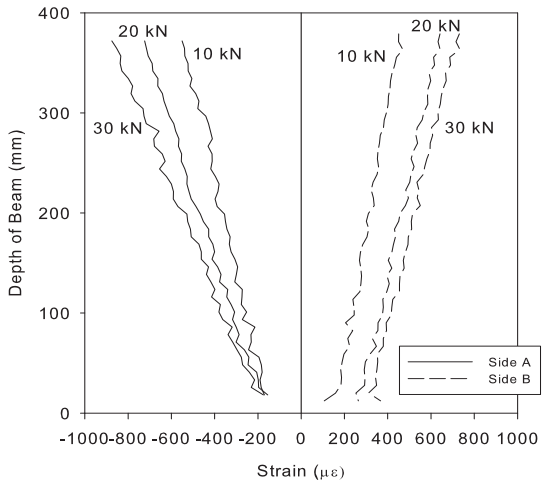

Figure 4: Beam 2 strain profile using DIC analysis at each load stage

Figure 5 also includes the strain profiles at each load stage using the external strain gauges and the FOS. Although the test was at constant temperature, the thermal effect on the fibre was determined over a 200 mm length of dummy fibre lying against the concrete but without epoxy. This dummy fibre was exposed to the same temperatures as the measurement fibre. This thermal strain from the dummy fibre was then subtracted from the measured FOS strain to obtain mechanical strain. The strain profiles obtained from the FOS were calculated by averaging the temperature corrected strain data over a 50 mm length of fibre at the same horizontal location as the strain gauges for both the top and bottom fibre, and a straight line was plotted between these two data points. The strain gauge readings are similarly plotted against the depth of the beam.

In both beams, the fibre optic strain profiles closely align with the strain gauge data, with a neutral axis close to 200 mm. However, the DIC averaged strain profiles do not match up with the strain gauge and fibre optic profiles. There seems to be a consistent error along the full height of the profile, which means that the slope of the DIC lines (the curvature) more closely matches the other two measurement techniques but the strain values themselves are not correct. Plotting the curvatures, in Figure 6, for each of the measurement techniques illustrates this improved correlation. Therefore, if the DIC strain profiles are forced through the neutral axis (200 mm) then the correlation between results significantly improves (Figure 7).

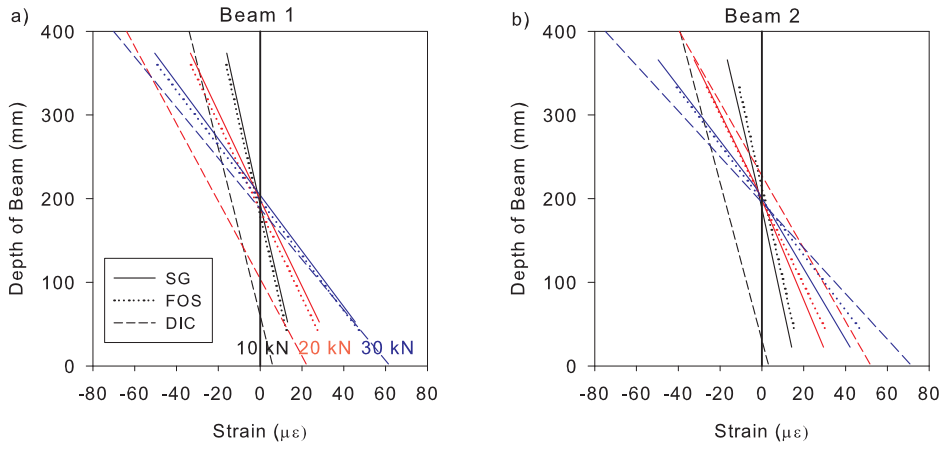

Figure 5: a) Beam 1 and b) Beam 2 strain profiles at each load stage

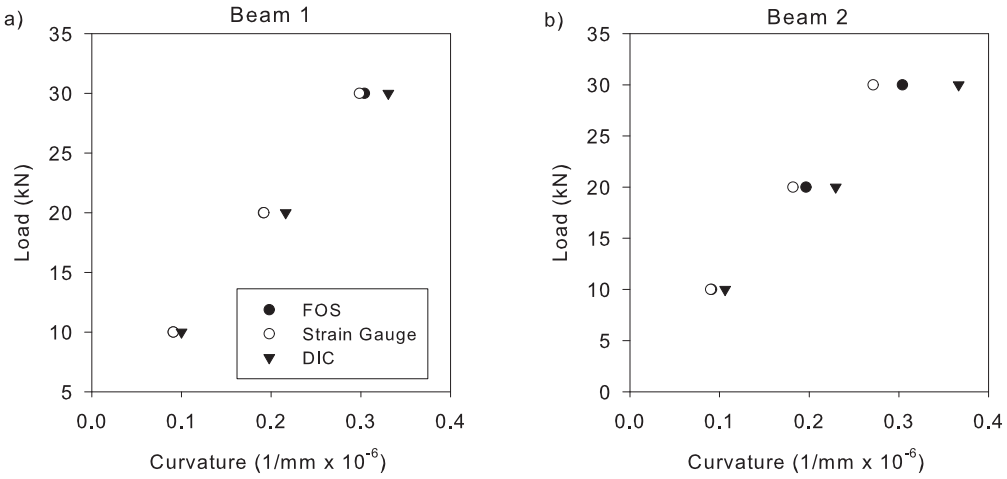

Figure 6: Curvatures measured by FOS, strain gauges and DIC for a) Beam 1 and b) Beam 2

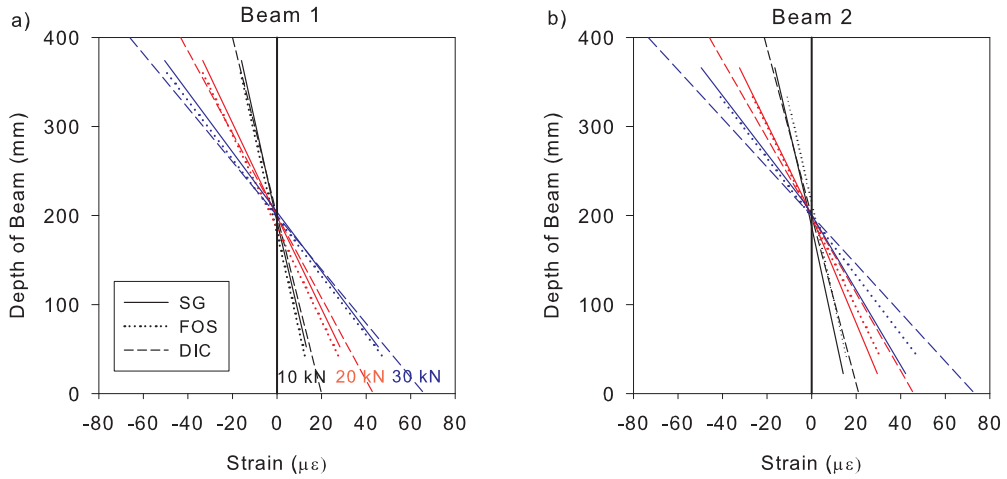

Figure 7: a) Beam 1 and b) Beam 2 strain profiles with shifted DIC data

Several factors could have contributed to this error. The FOS have a strain resolution as fine as 1 με (Luna, 2009; Kreger et al., 2006) while the DIC system has a theoretical strain resolution of less than 10 με (Hoult et al., 2013). For DIC, lens distortion can cause displacements to be measured slightly differently based on the location of the patch relative to the centre of the lens. Another factor could be that the cameras on different sides of the beam were at different heights, which would impact both out of plane and lens distortion effects. In addition, the face of the beam may not have been fully square on both sides meaning that rotation or translation on one side of the beam did not equal the same movement on the other side of the beam. These errors were amplified because the cameras were placed so close to the beam surface and the focal length of the lens was small. Temperature variations can also be a potential cause of strain error. Small temperature changes experienced by the camera during the test, despite the test being conducted at room temperature, could have caused a consistent strain error along the height of the beam. For example, self- heating of the camera can result in a 200 με error (Ma et al., 2012). Although, this normally takes approximately 2 hours for the camera to heat up to its maximum temperature that yields the largest error, during the 5 minutes it took to run this test, the camera could have increased in temperature by a few degrees even though a thermocouple monitoring the ambient temperature did not detect a substantial change in temperature.

5 CONCLUSIONS AND RECOMMENDATIONS

The results of this experimental study demonstrated that distributed FOS were effective at measuring strains in reinforced concrete beams loaded in four point bending when compared to conventional strain gauges. Although the DIC technique produced reasonable curvatures measurements, it was found that even small out of plane motion (rotation and translation) can cause significant error in DIC strain measurements. Placing two cameras on opposite sides and using the weighted average method, did not fully account for the strain error. It is suggested that further research should be conducted, because DIC can be an effective monitoring tool if adjustments are made for out of plane movement and temperature effects.

6 ACKNOWLEDGEMENTS

The authors gratefully acknowledge the financial support of the Natural Science and Engineering Research Council of Canada. The authors would also like to thank Mike Dutton, Keelin Scully, Ryan Regier and Paul Thrasher for their assistance with this research.

7 REFERENCES

Bao, X., DeMerchant, M., Brown, A., and Bremner, T. (2001). "Tensile and compressive strain measurement in the lab and field with the distributed brillouin scattering sensor." Journal of Lightwave Technology, 19(11), pp. 1698-1704.

Bisby, L. Take, W.A., and Caspary, A. (2007). "Quantifying strain variation in FRP confined concrete using digital image correlation: proof of concept and initial results." *Asia-Pacific Conference on FRP in Structure*.

Bourne-Webb, P. J., Amatya, B., Soga, K., Amis, T., Davidson, C., and Payne P. (2009). "Energy pile test at Lambeth College, London: geotechnical and thermodynamic aspects of pile response to heat cycles." Géotechnique, 59(3), pp. 237–248.

Casas, J.R., and Cruz, P.J.S. (2003). "Fiber optic sensors for bridge monitoring." Journal of Bridge Engineering, ASCE, 8(6), pp. 362-373.

Dutton, M. Hoult, N.A. and Take, W.A. 2011. "Towards a Digital Image Correlation based Strain Sensor," *Proc. of the International Workshop on SHM*, Stanford, Sept. 13 – 15.

Graybeal, B. A., Phares, B. M., Rolander, D. D., Moore, M. and Washer, G. (2003). Visual inspection of highway bridges, Journal of Nondestructive Evaluation, Vol. 21, No. 3, pp. 67-83.

Güemes, A., Fernández-Lopez, A., and Soller, B. (2010). "Optical fiber distributed sensing – physical principles and applications." Structural Health Monitoring, Sage Productions, 9(3), pp. 233-245.

Hoult, N.A., Take, W.A, Lee, C., and Dutton, M. (2013). "Experimental Accuracy of Two Dimensional Strain Measurements using Digital Image Correlation," Engineering Structures, 46, pp. 718-726.

Kreger, S.T., Gifford, D.K., Froggatt, M.E., Soller, B.J., and Wolfe, M.S. (2006). "High resolution distributed strain or temperature measurements in single- or multi-mode fiber using swept-wavelength interferometry." 18th Int. Conf. Opt. Fibre Sens. (OFS), Cancun, Mexico, 2006, Paper ThE42.

Lanticq, V., Gabet, R., Taillade, F., and Delepine-Lesoille, S. (2009). "Distributed optical fibre for structural health monitoring: upcoming challenges." *Optical Fibre, New Development,* Intech, Christophe Lethien, pp.177-199.

Lee, C., Take, W.A., and Hoult, N.A. "Theoretical Accuracy of Two Dimensional Strain Measurements using Digital Image Correlation," accepted to the ASCE J. of Computing in Civil Eng., Nov., 2011.

Luna Innovations Incorporated (2009). "OBR 4600 Data sheet." <http://www.lunatechnologies.com/products/software/files/OBR4600_Data_Sheet with Temp and Strain.pdf> (October 3, 2012).

Ma, S., Pang, J., and Ma, Q. (2012). "The systematic error in digital image correlation induced by self-heating of a digital camera." Measurement Science and Technology, 23, 7pp.

Sutton, M.A., Oreu, J.J., and Schreier, H.W. (2009). *Image correlation for shape, motion and deformation measurements*, Springer Science+Business Media, New York, NY.

White, D.J., Take, W.A, and Bolton, M.D. (2003). "Soil deformation measurement using particle image velocimetry (PIV) and photogrammetry." Géotechnique, 50(7), pp. 619-631.